Heliyon 8 (2022) e09442

Contents lists available at ScienceDirect

Heliyon

journal homepage: www.cell.com/heliyon

Research article

The effect of layering structures on mechanical and thermal properties of hybrid bacterial cellulose/Kevlar reinforced epoxy composites

R.A.A. Rusdi [a], N.A. Halim [a,*], N.M. Nurazzi [a], Z.H.Z. Abidin [b], N. Abdullah [a], F.C. Ros [a], N. Ahmad [a], A.F.M. Azmi [a]

[a] Centre for Defence Foundation Studies, National Defence University of Malaysia, Kem Sungai Besi, 57000, Kuala Lumpur, Malaysia
[b] Faculty of Science, University of Malaya, 50603, Kuala Lumpur, Malaysia

ARTICLE INFO

Keywords:
Bacterial cellulose
DMA
Layering structure
Low velocity impact
Kevlar
Polymer composites

ABSTRACT

The effect of layering structures on mechanical and thermal hybrid bacterial cellulose (BC) sheet/Kevlar reinforced epoxy composites was investigated. The BC sheet was extracted from Nata de Coco and used as green reinforcement material hybrid with Kevlar reinforced epoxy composites. The BC/Kevlar reinforced epoxy composite was fabricated by using hand lay-up technique equipped with vacuum bagging system and the BC sheets and Kevlar layers were laminated into different layered structures. The performance of the hybrid BC/Kevlar reinforced epoxy composites was characterized through tensile test and low velocity impact according to ASTM D3039 and ASTM D7136, respectively. The thermal performance of the hybrid composites was characterized by using dynamic mechanical analysis (DMA) test. Tensile test on BC sheet composites with Kevlar and epoxy demonstrated that the addition of BC sheet in BC/Kevlar could not withstand the tensor stress by reducing the tensile stress and Young's modulus. The one layer of Kevlar which was replaced with three to six BC sheets had increased the ability to absorb impact force. The storage modulus (E′) and Tan δ were significantly dependent on the number of BC sheets and its layering structure. The highest value of E′ was observed when BC sheets were arranged alternately with the Kevlar layers. Different damage mechanisms associated with the number of BC sheets and its layered-structure suggested that the BC sheet was functioning as an impact energy absorber as well as strengthening fibers. This study will upsurge interest in BC reinforced composites and the development of new ideas in automotive, marine and bullet applications.

1. Introduction

Conventional reinforcements such as glass fiber, Kevlar and carbon fiber have been widely used in the fabrication of structural polymer composite due to their numerous benefits, such as high strength, thermal stability and corrosion resistance [1]. From that, Kevlar had attracted noticeable attention and was reported to enhance various performances for structural applications. Furthermore, Kevlar has been reported to have some disadvantages, including non-recyclability, high cost, energy consumption, and a carcinogenic tendency [2]. Worldwide, researchers have developed biodegradable and renewable reinforcement for the composite structure to mitigate negative environmental consequences [3, 4, 5, 6]. Additionally, biodegradable and renewable reinforcements are less expensive than synthetic fibers and can be used in place of synthetic reinforcements. One of the most popular natural fiber reinforced polymer composites is plant lignocellulosic from the main component of plant cell walls like kenaf fiber [7, 8], sugar palm fiber [9, 10], bamboo [11, 12] and oil palm empty fruit bunch (OPEFB) fiber [13, 14]. These fibres are abundant with renewable characteristics and comes with unique mechanical and thermal performances [15, 16].

The ability to hybridized the two or more fibers or reinforcements in a single matrix by the hybridization of BC and Kevlar has increased performance, economies, and environmental benefits while maintaining the excellent mechanical performance of composites. Because BC sheets are biodegradable and lighter than Kevlar, it is feasible to balance more appealing performance features and the cost of composite systems when this material is used in automobiles, aerospace, or any other structural systems [15, 17, 18, 19, 20]. Intriguingly, it was reported that some specific bacteria can synthesize cellulose called bacterial cellulose. To remove the extractable fraction in cellulosic fiber, the pre-treatment associated with special solvent, chemicals and techniques is crucial. This method may cause slight damages to the fiber structure of cellulosic

* Corresponding author.
E-mail address: norhana@upnm.edu.my (N.A. Halim).

https://doi.org/10.1016/j.heliyon.2022.e09442
Received 5 November 2021; Received in revised form 6 February 2022; Accepted 11 May 2022

surface. In this regard, Nata de Coco which is BC produced from fermentation of coconut water called has a lot to offer. This BC is a white gelatinous cellulose, which is produced from the fermentation of *Acetobacter aceti Xylinum sp*. by using fruit juice as a medium. Nata de Coco is one of the most famous desserts in Asian countries, including the Philippines, Indonesia, Vietnam and Taiwan. It has high water content, which exceeds 90% with low calorific value, and has high fiber content. From the cell of Acetobacter bacterial BC, fibril with the length of several μm and width of 70 nm–100 nm are secreted [21]. Additionally, BC has a higher crystallinity and mechanical strength than plant cellulose, which has increased its use in biomedical and other related fields [22]. Many types of biocomposite based on PLA [23], starch [24], epoxy [25], PVA [26] have been fabricated by using BC as the biomaterial. These biocomposites are used in the treatment of wounds, burns, tissue regeneration, skin substitutes, food packaging and electronic devices.

Nakagaito et al. (2005) [27] impregnated BC pellicles sheets with phenolic resin to produce high-strength composites. The recorded composites' Young's modulus is higher than microfibrillated cellulose (MFC)-based composites, at 28 GPa compared to 19 GPa, respectively. This is due to exceedingly fine, pure, dimensionally uniform ribbon-like cellulose microfibril bundles arranged in a network of fairly straight, continuous alignment and the planar orientation obtained from the compression of BC pellicles into sheets. In order to increase the mechanical performance of glass fibre reinforced epoxy composites, Vu et al. (2017) had extracted BC as a green filler from Nata de Coco using a suspension in ethanol method [28]. The result shows that the BC loading at 0.3 wt.%, presented a critical role in boosting initial and propagation interlaminar fracture toughness by 128.8% and 1110%, respectively. Also, at 0.3 wt.%, the fatigue life of BC/glass fibre reinforced epoxy composites was enhanced by up to 12 times compared to an unmodified composite with BC as green filler. Montrikittiphant et al. (2014) [29] fabricated BC sheet reinforced PLA composites by laminating two thin PLA films onto a BC sheet. The tensile strength and modulus achieved 125 MPa and 6.9 GPa at a BC sheet loading of 65 vol.%.

Juntaro et al. (2012) a dried and well-consolidated BC sheet in PU resin, followed by UV crosslinking process for curing the composites [30]. Another study shows that the fabricated composites with the addition of BC in the form of pellicle or sheet networks may act as reinforcement in the mechanical structures of the composites. This by achieving optimum tensile strength and modulus at 151 MPa and 11.6 GPa at BC loading of 51 vol.%. To the best of our understanding, minimal studies have applied more than one sheet of BC as reinforcement or embedded with polymers, especially inter-layers with Kevlar. The mechanical performance of BC sheet reinforced epoxy laminated composites of 11 BC sheets has previously been studied. Still, the goal of this study was to evaluate the reinforcing effect of BC with wood-derived cellulose nanofibers [31]. In this work, BC sheet produced from Nata de Coco (*Acetobacter xyllinum*) was hybridized with Kevlar fabrics as reinforcement in epoxy composites. The hybrid composites were fabricated by using hand lay-up technique equipped with vacuum bagging system and the BC sheets and Kevlar layers were laminated into different layered structures. The performance of the composites was characterized through tensile test, low velocity impact test and DMA test.

2. Methodology

2.1. Materials

Nata de Coco (Figure 1 (a)) is a jelly-like food product that is produced by the fermentation of coconut water by using *Acetobacter xylinum* bacteria that was supplied by a local manufacturer in Selangor, Malaysia. Acetone used for cleaning was supplied by MERCK, Malaysia. Kevlar29 was purchased from Tazdiq Engineering Works, Malaysia, while EpoxyAmite 100 resin (Part A) and 102 medium hardeners (Part B) were supplied by DK Composites Sdn. Bhd., Malaysia. The mix ratio by volume between Part A and Part B was 3A:1B. The mixed specific gravity was 1.11 g/c.c with 650 cP of viscosity, 22 min of pot life and the cure time of the mixture was between 10 to 15 h.

2.2. Preparation of BC sheet

The raw Nata de Coco sample preparation process began by cleaning the raw sample, which included washing, soaking and rinsing with distilled water to remove any impurities. The washing and rinsing process was repeated twice daily until the pH of the rinsing water reached neutral (pH 5 to pH 7). Following that, the Nata de Coco was soaked in distilled water for 24 h to complete the cleaning process. These steps were repeated at room temperature for 1–2 weeks to neutralize and stabilize the pristine Nata de Coco. Then, the Nata de Coco was cut into 300 mm × 150 mm squares of an appropriate size to fit inside the oven cavity (as shown in Figure 2 (a)),. The wet sample (Figure 1 (b)) was slowly oven dried at 60 °C for 3–5 days. To prevent overheating of the sample, the oven temperature and sample condition were monitored continuously. Daily weights of the sample were taken during the drying process until its weight remained constant, indicating a density of 1.7 g/cm^3 to 1.8 g/cm^3. The constant weight indicated that the bacterial cellulose sheet was successfully dried. Finally, as illustrated in Figure 2 (b), the dried BC sheet was sealed in a zipped plastic bag and stored in a desiccator to prevent moisture absorption.

2.3. Composite fabrication technique

The hybrid composite fabrication started by cutting the BC sheet and Kevlar fabric according to the size of 30 cm (L) × 30 cm (W). Then the ceramic slab was carefully cleaned to remove dirt and dust by using acetone on its surface. The surface is sprayed with a silicone release agent for composite ease removal and to avoid any stacking with the composites. Part A and Part B were mixed using the given weight ratio, 3A:1B, followed by stirring the resin mixture until the color changed from light white to clear yellow. The resin mixture was applied by evenly brushing it in one direction on the first layer of composite materials, either BC sheet or Kevlar fabric. The composite layer was moistened with epoxy resin and carefully placed on the ceramic slab to avoid voids

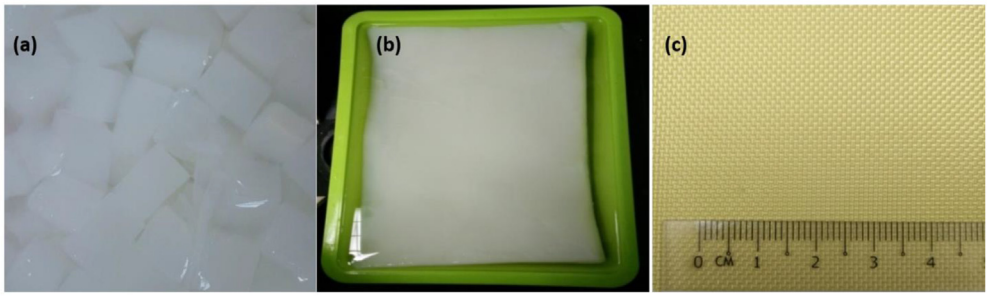

Figure 1. (a) Nata de Coco jelly used in this study, (b) the BC sheet formed and (c) Kevlar fabric.

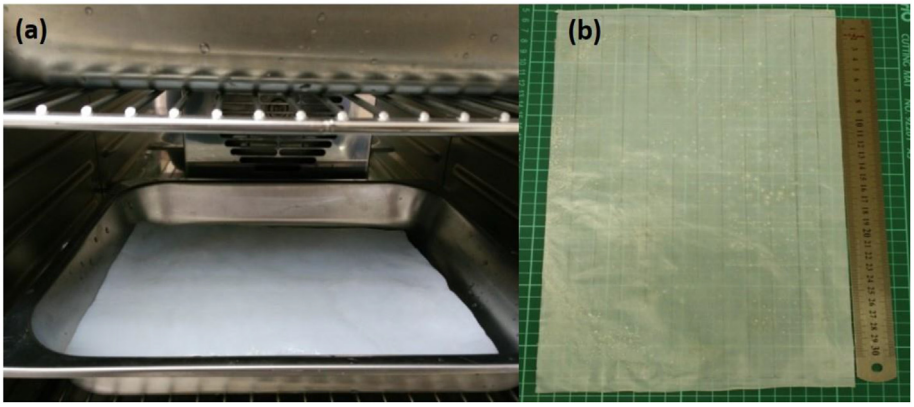

Figure 2. (a). Oven drying process and (b) Dried BC sheet sample.

between the slab surface and layer. A roller was also used to remove any voids by rolling them up and down throughout the sample surface. This process was repeated until the required number of composite layers was obtained. The next step was to install a vacuum bagging system, as demonstrated in Figure 3 (a) and Figure 3 (b), respectively.

To begin, a layer of peel ply was placed on top of the sample, followed by a perforated release fabric and breather fabric to trap and hold excess resin during the vacuum process. After carefully spreading a vacuum bagging film over the sample, it was tapped to the sealant tapes surrounding it. It was critical to stretch the plastic film evenly to avoid wrinkles on the surface of sample when the vacuum pump was applied. After 2 h of vacuum process, the vacuum bagging system was left at room temperature for an additional 24 h Table 1 shows the specification and corresponding layering of BC and Kevlar for the composites structure.

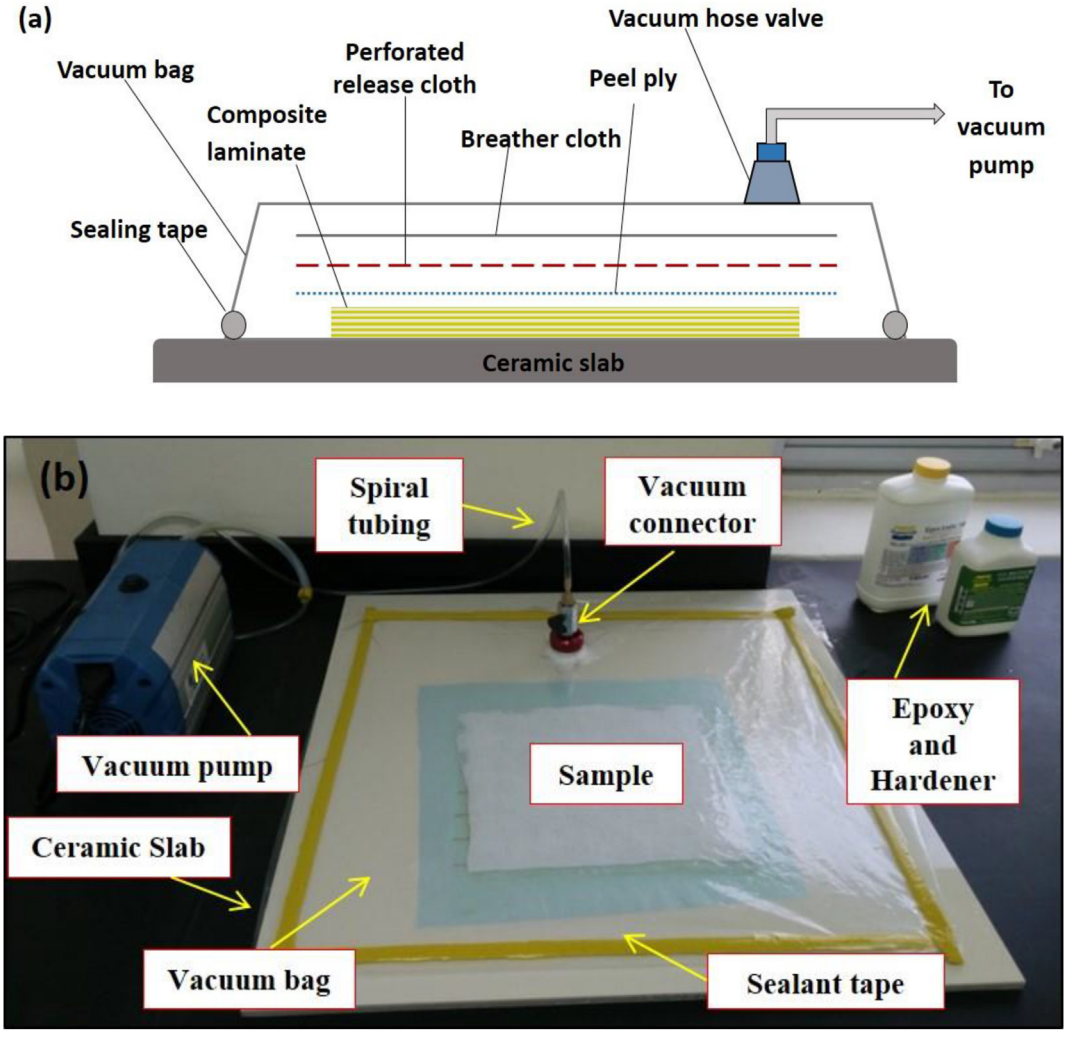

Figure 3. (a) Schematic diagram of composite preparation and (b) the actual set-up.

Table 1. Specification and corresponding layering of BC sheet and Kevlar reinforced epoxy composites.

Sample	Composite acronyms	No. of layers		Schematic layering sequence
		BC sheet	Kevlar fabric	
Pristine sheet BC	BC	1	-	
Pristine Kevlar fabric	K	-	1	
BC sheet with epoxy	BC/EP	1	-	
Kevlar fabric with epoxy	K/EP	-	1	
3 layers of Kevlar fabric	K/K/K	-	3	
2 layers of Kevlar fabric with 1 BC sheet	K/BC/K	1	2	
3 layers of BC sheet with 2 layers of Kevlar fabric	BC/K/BC/K/BC	3	2	
2 layers of Kevlar fabric with 3 layers of BC sheet	K/3BC/K	3	2	
2 layers of Kevlar fabric with 6 layers of BC sheet	K/6BC/K	6	2	
2 layers of Kevlar fabric with 6 layers of BC sheet with different sheet arrangements	2BC/K/2BC/K/2BC	6	2	
2 layers of Kevlar fabric as the middle core with 6 layers of BC sheet	3BC/2K/3BC	6	2	

2.4. Characterizations

The tensile test was performed using Instron model 5569A (USA) with a capacity of 50 kN test machine according to ASTM D3039. The dimensions of the samples were 250 mm (L) x 160 (W) mm. The gauge length was 200 mm, with a crosshead speed of 5 mm/min applied for the test. The tensile stress (σ), strain (ε) and Young's modulus (E) was calculated according to Eq. (1), Eq. (2) and Eq. (3), respectively [32]. For each sample, seven repetitions were performed and the average was then reported.

$$\sigma = \frac{F}{A}\left(\mathrm{N}/\mathrm{m}^2\right) \tag{1}$$

where, F is a force and A is cross-sectional area of sample.

$$\varepsilon = \frac{\Delta L}{L} \times 100(\%) \tag{2}$$

where, ΔL is total elongation and L is original length of sample.

$$\mathrm{E} = \frac{\sigma}{\varepsilon}\left(\mathrm{N}/\mathrm{m}^2\right) \tag{3}$$

where, σ is tensile stress and ε is strain of sample.

The low velocity impact test was conducted following ASTM D7136 by using a CEAST 9350 machine with the tup holder mass of 4.3 kg and tup nominal mass was 1.2 kg. The dimension of sample was 50 mm (L) × 50 mm (W). The impact tests were conducted at room temperature under different impact energy values that ranged from 3 J, 6 J and 9 J from a 4.3 kg indenter collision. It has a 20 mm diameter hemispherical impact head and was released at an initial velocity of 1.8 m/s. Testing started when the hydraulic actuator dropped an impactor with a round nose tip of about 20 mm in diameter. Impact resistance was studied by examining the condition of a tested sample and its curves in the force versus time or f-t (f-t) plot, velocity versus time (v-t) plot and force versus impact displacement (f-d) plot. Different curves in these plots demonstrated indenter penetration, impact absorption, impact resistance and bounced-back effect. From the v-t plot, kinetic energy (E_k) of the indenter and impact force (F) can be calculated according to Eq. (4) and Eq. (5), respectively [33]. Where m, v, d is mass, velocity and displacement, respectively. For each sample, three repetitions were performed and the average was then reported.

$$\mathrm{E_k} = \frac{1}{2}mv_f^2 - \frac{1}{2}mv_i v^2(\mathrm{J}) \tag{4}$$

$$= \frac{E_k}{d}(\mathrm{J/mm}) \tag{5}$$

DMA 8000 from PerkinElmer instrument was used for the evaluation of dynamic mechanical thermal behaviors of the BC/Kevlar composite. Specimens of size 30 mm (L) x 10 mm (W) were used for the DMA under three-point bending mode at an oscillation frequency of 1 Hz. The temperature was ramped from 30 °C to 100 °C under a controlled sinusoidal force with a heating rate of 5 °C/min. The Tan δ, storage modulus (E') over loss modulus (E") was calculated according to Eq. (6) [34].

$$\mathrm{Tan}\,\delta\frac{\mathrm{E''}}{\mathrm{E'}} \tag{6}$$

3. Results and discussion

3.1. Tensile properties

Table 2 shows the tensile stress, tensile modulus and strain of the BC sheet/Kevlar reinforced epoxy composites. The highest tensile stress was observed for K/K/K composites sample with 331 MPa, followed by BC/K/BC/K/BC and the lowest one was BC/EP composites, which were 266 MPa and 25 MPa, respectively. It was observed that in general the incorporation of BC sheet in hybrid composite reduced the tensile stress

Table 2. Tensile properties of hybrid BC sheet/Kevlar reinforced epoxy composites.

Sample	Tensile Stress (MPa)	Young's Modulus (GPa)	Elongation at Break (%)
BC	167.64 (1.13)	12.78 (0.54)	5.20 (0.30)
K	231.56 (1.09)	14.51 (0.31)	33.64 (0.31)
BC/EP	24.59 (1.07)	3.77 (0.25)	2.25 (0.20)
K/EP	104.16 (3.17)	2.69 (0.22)	36.58 (0.29)
K/K/K	331.38 (2.52)	10.22 (0.24)	19.88 (0.15)
K/BC/K	194.89 (2.25)	5.52 (0.35)	23.61 (0.30)
BC/K/BC/K/BC	266.23 (3.36)	8.13 (0.23)	20.92 (0.19)
K/3BC/K	161.17 (3.52)	4.91 (0.25)	19.42 (0.31)
2BC/K/2BC/K/2BC	166.32 (3.57)	5.83 (0.41)	38.73 (0.50)
K/6BC/K	167.76 (1.37)	5.42 (0.29)	18.21 (0.33)
3BC/2K/3BC	118.87 (1.39)	5.83 (1.10)	31.56 (0.90)

(*) = Standard deviation.

and Young's modulus properties. However, the presence of BC sheet could increase the elongation at break of the hybrid composites. The five composites, which were 2BCK2BCK2BC, 3BCK3BC, KBCK and BCKBCKBC, showed higher elongation at break than that of KKK (20%) composite with 39%, 31.56%, 24% and 21%, respectively. Furthermore, the BCKBCKBC composites had higher tensile stress than the KBCK composite sample because an effective layering design of balance (BC/K/BC/K/BC) designed between the outer layer of the composite BC sheet's skin and a continuous layer of Kevlar performed as a core and tendon for the composite structure, rather than layering from the K/BC/K. The possibility of individual BC sheets inhibited the microcrack propagation into the composites' core at the outer surface, the composites' effective layering and structural design avoided sudden and rapid crack growth. Additionally, an optimum loading of epoxy matrix acted as a binder of the BC sheet and Kevlar, efficiently transfer the load to the core structure and providing rigidity and shape to the structure. This resulted to the enhancement of the mechanical performance of composites [15].

Besides, results found that the hybrid composites for K/3BC/K, 2BC/K/2BC/K/2BC, K/6BC/K and 3BC/2K/3BC showed tensile stress around 118 MPa and 160 MPa, tensile modulus from 4.9 GPa to 5.8 GPa. However, the elongation at break for composite sample 2BC/K/2BC/K/2BC achieved the highest elongation at break. Based on the results, each layer consisted of two sheets of BC contained in the composite led to higher elongation at break. This was due to the ductility enhancement when the layering design placed two sheets of BC on each layer that supported and prolonged the plastic deformation for the composite failure. Besides, the synergistic effect of the BC sheet was observed when the BC sheet was placed as a skin or outer layer for the composite structure and Kevlar as a core. This was observed at composite samples BC/K/BC/K/BC and 3BC/2K/3BC for better elongation at break and tensile modulus as compared to composite sample K/BC/K, whereby Kevlar was an outer layer. Overall, compared with tensile properties of K/K/K reinforced epoxy composites, the composite sample with BC sheet as an outer layer showed a better result; it was either for tensile stress, tensile modulus or elongation at break, especially for BC/K/BC/K/BC composites.

3.2. Low velocity impact properties

In low velocity impact properties, the penetration, impact absorption, impact resistance and bounced-back effect of BC sheet/Kevlar reinforced epoxy composite will be studied. The application of impact energy at 3 J on BC sheet reinforced epoxy composite sample caused penetrations of the impact through-thickness with splitting on the rear end face. Penetration occurs in materials that cannot withstand the impact energy. Figure 4 (a–d) shows damage patterns on hybrid BC sheet/Kevlar reinforced epoxy composites in terms of penetration, impact absorption, impact resistance and bounce back. A linear increase in the muzzle velocity demonstrated poor resistance of the samples but not in the case of impact absorption (Figure 4 (b)). For example, even though K/3BC/K 3 J sample had a linear v-t plot, Table 3 describes that this sample was able to absorb impact without any penetration. From the v-t plot, kinetic energy, Ek during collision was about +3230 mJ. This positive energy implied that work was done on the system, whereby the tested material entered or absorbed energy. In other words, the indenter movement experienced minimal resistance force that could not slow it down.

Strong Kevlar fabric was able to endure the impact force, but flexibility in the fabric allowed this sample to slip from its holder during a collision with the indenter. Kevlar reinforced epoxy composites sample that showed a damage pattern in Figure 4 (c) demonstrated that the impact resistance by the composite sample had higher rigidity than pristine Kevlar fabric with an application of 3 J impact energy resulted in the peak force of about 501 N. From the v-t plot, collision with the indenter produced kinetic energy, Ek of about -2360 mJ. This negative kinetic energy indicated that the system had worked, whereby the composite absorbed impact energy and indenter lost its energy. In other words, the indenter movement faced resistance force that could slow it down.

An increase in Kevlar layers of the K/K/K composite gave better rigidity with a bell-curve peak (bounced-back) in Figure 4 (d), and the impact force was about 862 N. It caused the indenter to bounce back after the collision. The effect of bounced-back can be observed in Figure 4 (d) with the hysteresis curve on the f-d plot. The f-d plot demonstrates that the elasticity in Kevlar can absorb impact energy during a collision. Kevlar fabric may store the elastic potential energy before being released to regain its original condition. When the impact energy was raised to 9 J, the result showed that it increased the impact force of the K/K/K sample to 1490 N and this sample had traits of material resistance to impact but without the bounced-back effect. It demonstrated the plastic behavior of Kevlar fabric under high impact energy.

Table 3 lists the impact force of tested samples and condition for BC sheet/Kevlar reinforced epoxy composites. From Table 3, replacing one layer of Kevlar with a BC sheet caused the impact force of K/BC/K composite to reduce up to 41.34%. Like the K/K/K composite, this sample showed the elastic property at low impact energy. A viscous elastic effect was observed when the impact energy was increased to 6 J and 9 J. BC sheet in this sample helped to absorb the impact energy before it reached the Kevlar layer at the bottom. Additional of 2 BC sheets in BC/K/BC/K/BC composite also resulted in the viscous elastic behavior at 9 J impact energy. While at 3 J, this sample had elastic behavior and demonstrated a significant increase in an impact force of about 43%. A sheet of BC on the impacted side helped to strengthen the composite sample.

Moreover, the role of the BC sheet as an energy absorber can also be seen in the case of K/3BC/K, K/6BC/K, 3BC/2K/3BC and 2BC/K/2BC/K/2BC composite samples. In each case, energy absorption gave the viscous elasticity and reduced the impact force of around 41%–96%. When impact energy increased from 3 J to 9 J, the trend for low-velocity impact properties of K/K/K, K/BC/K and BC/K/BC/K/BC changed from elastic to viscoelastic. However, such trend reversed when the thickness of the BC phase was increased in the composites. The K/3BC/K, K/6BC/K, 3BC/2K/3BC and 2BC/K/2BC/K/2BC composites demonstrated viscoelasticity at 3 J and changed to elasticity at 9J impact energy.

To some extent, the high crystallinity in BC helped in energy dissipation upon collision with the indenter. As strengthening fibres in the BC/Kevlar composites, 3-layer and 6-layer additions of BC sheet had increased the impact force from 41% to 197%. Extensive networks formed by interlocking cellulose fibrils could store and release impact energy to regain its original shape. In the plastic region, resistance to impact could cause permanent deformation on such network structures. Results showed that the BC sheet had excellent potential as reinforcement in the Kevlar composite, reducing the number of Kevlar layers in

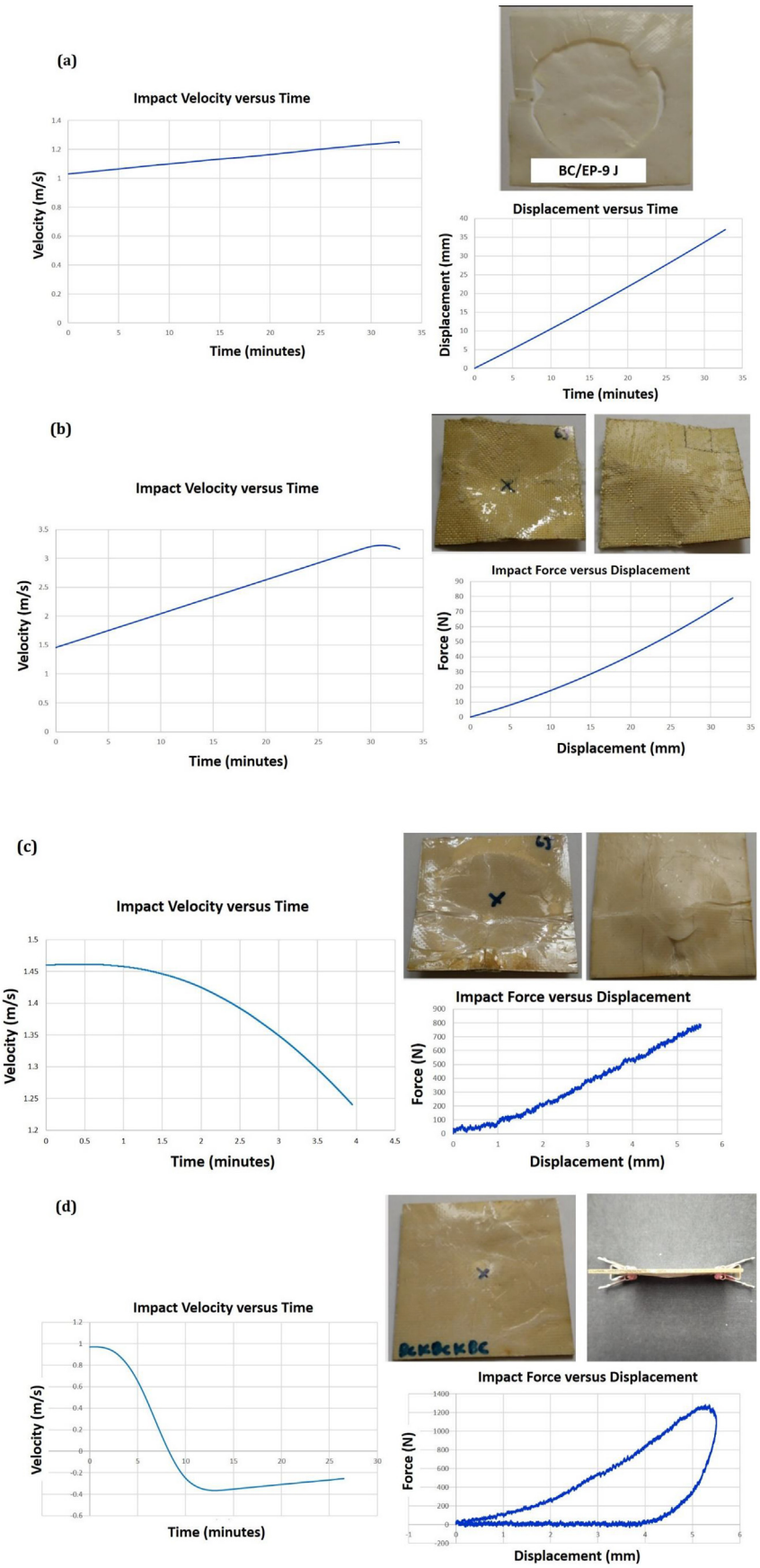

Figure 4. Damage pattern on hybrid BC sheet/Kevlar reinforced epoxy composites in terms of (a) penetration, (b) impact absorption, (c) impact resistance and (d) bounce back.

the composite. Due to the number of BC sheets and their layered structures, different damage mechanisms showed that BC sheets functioned as an impact energy absorber. It could give crucial additional support in the BC sheet/Kevlar composites when struck by the impactor [35].

3.3. Dynamic mechanical analysis properties

The effects of temperature on glass transition temperature (Tg) that formed the peak of Tan δ, E′ and Tan δ for hybrid BC/Kevlar composites are presented in Table 4. The maximum energy stored in the materials during the oscillation cycle is represented by E′ peaks, which described the stiffness of samples [5]. The replacement of one Kevlar layer with a BC sheet showed a significant increase in the storage E′ and improved the elasticity of K/BC/K composite. Elasticity in this sample explained its comparatively low viscoelasticity. However, the thickness increase of the BC phase improved the Tan δ peaks for K/3BC/K, K/6BC/K, 3BC/2K/3BC and 2BC/K/2BC/K/2BC composites around temperature 55 °C. The improved viscoelasticity means that these composites were able to absorb and dissipate energy throughout their structures [36].

Table 4 shows the Tg, E′ and Tan δ versus temperature for K/K/K, K/BC/K, K/3BC/K, BC/K/BC/K/BC, 2BC/K/2BC/K/2BC, K/6BC/K and 3BC/2K/3BC hybrid composites. The Tg of a composite can be obtained from the peak maximum of either the E′ or the Tan δ curve. Yet to calculate Tg value, the maximum peak in the Tan δ plot is more definite than the imprecise positioning of tangents [37]. The higher Tg indicates larger the cross-linked density, which then leads to higher composites modulus value of the composites structure. Previous study stated that Kevlar fabrics reinforced composites might increase E′ due to the stiffening effect of Kevlar reinforced epoxy matrix and finally decreased the damping curve of polymer matrix [38]. Idicula et al. (2005) [39] stated a lower damping value related to Tg that presents a better load-bearing properties due to improvement in interfacial adhesion between the reinforcement with the matrix itself. The enhanced interfacial adhesion had limited the intermolecular movement of the polymeric chain, caused for a reduction in the damping factor. Referring to Aziz et al. (2005) [40], the decrease of the Tan δ peak is contributed by the integration of stiff fibers limiting the movement of the polymer molecules. Thus, it provided excellent damping resistance in the composite structures.

The Tg of the composites ranged from 50.39 °C to 70.26 °C. The shift of Tg values to a higher temperature resulted from the impact when the BC sheet was arranged alternately with the Kevlar layer. This tended to restrict the chain mobility of the epoxy. However, the Tg of the epoxy composites was 55 °C (Table 4), which was lower than the Tg of the BC sheet/Kevlar reinforced epoxy composite. This was because the impact of the increased thermal stability donated by lamination from the BC sheet and Kevlar fabrics. From the K/K/K composite, the E′ was about 408 MPa at maximum Tan δ. When the layer of Kevlar fabric was replaced with a layer of BC sheet, the E′ of K/BC/K composites increased to 639 MPa indicated 56% of increment. The three-layers of Kevlar fabrics composite were more rigid as compared to that of K/BC/K sample. The BC/K/BC/K/BC composite had an E′ of 1120 MPa. This value increased to 174% when a layer of Kevlar was replaced with three layers of BC sheets. The improved E′ implied elasticity, which was aligned with the elastic behavior observed in the low velocity impact study for this composite. However, three layers of BC sheet seemed to decrease the E′ of K/3BC/K sample but it increased the Tan δ to 0.295. The 17% reduction in elasticity was consistent with the increase in viscoelasticity. Previous section in low velocity impact properties revealed similar remark, whereby increased BC phase thickness changed the elastic-to-viscoelastic trait to viscoelastic-to-elastic behavior with the increased impact energy.

The BC sheet as a core in K/BC/K gave higher E′ with 639 MPa as compared to the 348 MPa from the three-layered BC sheet core in K/3BC/K. Again, higher thickness in BC phase caused the change from elasticity to viscoelasticity. 3BC/2K/3BC sample drew 630 MPa of E′, which was similar to that of K/BC/K. From this point of view, BC sheet as the core in BC/Kevlar composite demonstrated a better layered-structure to gain elasticity. Therefore, BC sheet has great potential to decrease the number of Kevlar layers in composites with the ratio of one layered Kevlar replaced with three layers of BC sheet.

The damping factor of a composite is affected by interfacial interactions in the composite. A low damping value in a Tan δ plot represents enhanced interfacial interactions, while comparatively higher Tan δ

Table 3. Impacted force and hybrid BC sheet/Kevlar reinforced epoxy composites condition.

Sample	Impact energy (J)	Peak Force (N)	Sample condition	Composite performance (%)	Kinetic Energy, (E_k) (J)
BC	3J	48 (0.11)	Penetrate		-0.35
	6J	Vague			-0.24
	9J	43 (0.09)			-0.15
BC/EP	3J	36 (0.12)	Penetrate		-0.17
	6J	Vague			-0.15
	9J	43 (0.15)			-0.17
K	3J	113 (0.02)	Slipped		-1.21
	6J	Vague			-0.03
	9J	43 (0.02)			-0.17
K/EP	3J	501 (0.14)	Slightly Resist		-2.36
	6J	48			-0.16

		(0.15)			
	9J	51 (0.12)			-0.14
K/K/K	3J	862 (0.10)	Bounced		-2.68
	6J	775 (0.09)	Resist		-0.09
	9J	1490 (0.14)	Resist		-4.34
K/BC/K	3J	850 (0.15)	Bounced	↓1.4 when replace 1K with 1BC	-2.60
	6J	424 (0.13)	Absorb	↓45.3	6.18
	9J	874 (0.17)	Absorb and resist	↓41.3	0.02
BC/K/BC/K/BC	3J	1240 (0.21)	Bounced	↑43.0 with different series arrangement of replacing 3BC with 1K	-0.29
	6J	1266 (0.19)	Resist	↑41.0	-0.15
	9J	904 (0.15)	Absorb and Resist	↓60.8	11.58
K/3BC/K	3J	40 (0.22)	Absorb	↓95.4 when replace 1K with 3BC	3.23
	6J	223 (0.17)	Absorb	↓71.2	0.38
	9J	2308 (0.19)	Bounced	↑62.1	- 0.83
K/6BC/K	3J	55 (0.15)	Absorb	↓93.6 when replace 1K with 6BC	0.00
	6J	1798 (0.19)	Resist	↑132	-0.93
	9J	2512 (0.20)	Bounced	↑68.5	-12.81
3BC/2K/3BC	3J	36 (0.20)	Absorb	↓95.8 when replace 1K with 6BC	0.00
	6J	1621 (0.15)	Resist	↑109	-1.55
	9J	1876 (0.18)	Bounced	↑25.9	-12.10
2BC/K/2BC/K/2BC	3J	200 (0.15)	Absorb	↓76.8 when replace 1K with 6BC	0.24
	6J	2304 (0.20)	Resist	↑197	-0.63
	9J	2344 (0.17)	Bounced	↑57.3	-9.94

(*) = Standard deviation.

value specifies the lack of interfacial adhesion [41]. Table 4 shows composites with a comparatively thicker BC phase had higher Tan δ than that of composites with thin BC phase. In this work, thick BC sheet phase reduced the interfacial adhesion with Kevlar layers. Meanwhile, a thin layer of BC sheet in between the Kevlar layers interacted better to storage energy. Overall, the DMA properties of hybrid BC/Kevlar composites were significantly dependent on the number of BC sheets and Kevlar layers as well as their layering sequence structure. The E′ of composites with three-layer structure of BC sheet showed the highest value when BC sheet was arranged alternately with Kevlar layer. Such arrangement helps for better storage energy with improved interactions at the BC-Kevlar interphase. DMA analysis also confirmed the elastic and viscoelastic behaviors observed in the low velocity impact study.

Table 4. Tan δ and E′ of hybrid BC/Kevlar composites.

Sample	Tg from Tan δ (°C)	Tan δ	Storage Modulus (E′) (MPa)	Storage modulus percentage performance of composite compared to K/K/K composite (%)
K/K/K	63.73	0.271	408	-
K/BC/K	69.90	0.235	639	+56
BC/K/BC/K/BC	70.26	0.223	1120	+174
K/3BC/K	56.78	0.295	348	-17
2BC/K/2BC/K/2BC	59.49	0.344	381	-6
3BC/2K/3BC	65.97	0.298	630	+54
K/6BC/K	50.39	0.254	205	-49

4. Conclusion

In conclusion, the tensile test on the BC sheet showed that it has high tensile stress with 167.64 MPa and a Young's modulus of 12.78 GPa, but low in the elongation at break with 5.2%. Tensile test on BC sheet composites with Kevlar and epoxy demonstrates that the addition of BC sheet in BC/Kevlar cannot withstand the tensor stress. Such interrupted phase limits stress dissipation in the polymers and close-packed structures of BC restrict epoxy resin to form continuous phase through-thickness on BC sheet by reducing the tensile stress and Young's modulus down to 63% and 52%, respectively. The low-velocity impact study showed that BC/Kevlar composite could endure the impact energy of 3 J–9 J during the tests. Analysis on the f-t, v-t and f-d plots and the condition of tested samples revealed the elastic, viscoelastic, plastic behavior of composites and signified damage mechanisms under impact stress: penetration, impact absorption, impact resistance bounced-back effect. Replacement of 1 Kevlar layer with 3 BC sheets in the alternating structure of BC/K/BC/K/BC increased the impact force by 43%. High crystallinity means that BC chains were well aligned, which were strongly held by covalent and hydrogen bonds. Therefore, it produced strong nanofibrils that interlock in the web-like structure, which was significantly helpful to absorb impact energy. Due to the number of BC sheets and their layered structures, different damage mechanisms suggested that BC sheets functioned as impact energy absorbers and reinforcing materials. The DMA on BC sheet/Kevlar composites confirmed the elastic and viscoelastic behaviors observed in the low-velocity impact analysis. The E′ and Tan d were significantly dependent on the number of BC sheets and Kevlar layers as well as their layered structure. The BC/K/BC/BC composite showed the highest E′ value when the BC sheet was arranged alternately with the Kevlar layer. This arrangement helped to store energy better with improved interactions at the BC-Kevlar interphase.

Declarations

Author contribution statement

R.A.A. Rusdi: Conceived and designed the experiments; Performed the experiments; Analyzed and interpreted the data; Wrote the paper.

N.A. Halim: Conceived and designed the experiments; Analyzed and interpreted the data; Contributed reagents, materials, analysis tools or data; Wrote the paper.

N.M. Nurazzi: Analyzed and interpreted the data; Wrote the paper.

Z. H. Z. Abidin, F. C. Ros: Conceived and designed the experiments; Analyzed and interpreted the data.

N. Abdullah: Analyzed and interpreted the data.

N. Ahmad, A.F.M Azmi: Conceived and designed the experiments.

Funding statement

This work was supported by Centre for Research Management and Innovation, Universiti Pertahanan Nasional Malaysia (UPNM) and The Ministry of Higher Education under the Niche Research Grant Scheme (NRGS) (grant: NRGS/2013/UPNM/PK/P1).

Data availability statement

Data included in article/supplementary material/referenced in article.

Declaration of interests statement

The authors declare no conflict of interest.

Additional information

No additional information is available for this paper.

References

[1] N. Mohd Nurazzi, et al., A review: fibres, polymer matrices and composites, Pertanika J. Sci. Technol. 25 (4) (2017).
[2] S.H. Park, Types and health hazards of fibrous materials used as asbestos substitutes, Safet. Health Work 9 (3) (2018) 360–364.
[3] N. Khundamri, et al., Bio-based flexible epoxy foam synthesized from epoxidized soybean oil and epoxidized mangosteen tannin, Ind. Crop. Prod. 128 (2019) 556–565.
[4] H.A. Aisyah, et al., A comprehensive review on advanced sustainable woven natural fibre polymer composites, Polymers 13 (3) (2021) 471.
[5] M.H. Zin, et al., Automated spray up process for Pineapple Leaf Fibre hybrid biocomposites, Compos. B Eng. 177 (2019) 107306.
[6] R.A. Ilyas, et al., Potential of natural fibre composites for transport industry: a review, in: Prosiding Seminar Enau Kebangsaan, Persatuan Pembangunan dan Industri Enau Malaysia (PPIEM) Bahau, Negeri, 2019.
[7] N. Soatthiyanon, C. Aumnate, K. Srikulkit, Rheological, tensile, and thermal properties of poly (butylene succinate) composites filled with two types of cellulose (kenaf cellulose fiber and commercial cellulose), Polym. Compos. 41 (7) (2020) 2777–2791.
[8] M.R.M. Asyraf, et al., Dynamic Mechanical Behaviour of Kenaf Cellulosic Fibre Biocomposites: A Comprehensive Review on Chemical Treatments, Cellulose, 2021, pp. 1–21.
[9] R.A. Ilyas, et al., Effect of hydrolysis time on the morphological, physical, chemical, and thermal behavior of sugar palm nanocrystalline cellulose (Arenga pinnata (Wurmb.) Merr), Textil. Res. J. 91 (1-2) (2021) 152–167.
[10] R.A. Ilyas, et al., Sugar palm (Arenga pinnata [Wurmb.] Merr) starch films containing sugar palm nanofibrillated cellulose as reinforcement: water barrier properties, Polym. Compos. 41 (2) (2020) 459–467.
[11] C.J. Wijaya, et al., Hydrophobic modification of cellulose nanocrystals from bamboo shoots using rarasaponins, ACS Omega 5 (33) (2020) 20967–20975.
[12] B. He, et al., Structural and physical properties of carboxymethyl cellulose/gelatin films functionalized with antioxidant of bamboo leaves, Int. J. Biol. Macromol. 164 (2020) 1649–1656.
[13] D.S. Lai, et al., On the use of OPEFB-derived microcrystalline cellulose and nano-bentonite for development of thermoplastic starch hybrid bio-composites with improved performance, Polymers 13 (6) (2021) 897.
[14] F. Ismail, et al., Influence of sulphuric acid concentration on the physico-chemical properties of microfibrillated cellulose from oil palm empty fruit bunch fibre, J. Oil Palm Res. 32 (4) (2020) 621–629.
[15] N.M. Nurazzi, et al., Development of sugar palm yarn/glass fibre reinforced unsaturated polyester hybrid composites, Mater. Res. Express 5 (4) (2018) 45308.
[16] A.G.N. Abbas, et al., Kenaf fibre reinforced cementitious composites, Fibers 10 (1) (2022) 3.
[17] N.M. Nurazzi, et al., Thermal properties of treated sugar palm yarn/glass fiber reinforced unsaturated polyester hybrid composites, J. Mater. Res. Technol. 9 (2) (2020) 1606–1618.
[18] N.M. Nurazzi, et al., Curing behaviour of unsaturated polyester resin and interfacial shear stress of sugar palm fibre, J. Mech. Eng. Sci. 11 (2) (2017) 2650.
[19] N.M. Nurazzi, et al., A review on mechanical performance of hybrid natural fiber polymer composites for structural applications, Polymers 13 (13) (2021) 2170.
[20] N.M.Z.N. Baihaqi, et al., Effect of fiber content and their hybridization on bending and torsional strength of hybrid epoxy composites reinforced with carbon and sugar palm fibers, Polimery 66 (1) (2021) 36–43.
[21] Y.K. Noh, et al., Fabrication of bacterial cellulose-collagen composite scaffolds and their osteogenic effect on human mesenchymal stem cells, Carbohydr. Polym. 219 (2019) 210–218.
[22] W.K. Czaja, et al., The future prospects of microbial cellulose in biomedical applications, Biomacromolecules 8 (1) (2007) 1–12.
[23] J.J. Blaker, et al., Aligned unidirectional PLA/bacterial cellulose nanocomposite fibre reinforced PDLLA composites, React. Funct. Polym. 85 (2014) 185–192.
[24] H. Abral, et al., Antimicrobial edible film prepared from bacterial cellulose nanofibers/starch/chitosan for a food packaging alternative, Int. J. Polym. Sci. 2021 (2021).

[25] S. Le Hoang, et al., Preparation and physical characteristics of epoxy resin/bacterial cellulose biocomposites, Polym. Bull. 75 (6) (2018) 2607–2625.
[26] D. Aki, et al., 3D printing of PVA/hexagonal boron nitride/bacterial cellulose composite scaffolds for bone tissue engineering, Mater. Des. 196 (2020) 109094.
[27] A.N. Nakagaito, S. Iwamoto, H. Yano, Bacterial cellulose: the ultimate nano-scalar cellulose morphology for the production of high-strength composites, Appl. Phys. A 80 (1) (2005) 93–97.
[28] C.M. Vu, et al., Environmentally benign green composites based on epoxy resin/bacterial cellulose reinforced glass fiber: fabrication and mechanical characteristics, Polym. Test. 61 (2017) 150–161.
[29] T. Montrikittiphant, et al., Bacterial cellulose nanopaper as reinforcement for polylactide composites: renewable thermoplastic nanopapreg, Macromol. Rapid Commun. 35 (19) (2014) 1640–1645.
[30] J. Juntaro, et al., Bacterial cellulose reinforced polyurethane-based resin nanocomposite: a study of how ethanol and processing pressure affect physical, mechanical and dielectric properties, Carbohydr. Polym. 87 (4) (2012) 2464–2469.
[31] K.Y. Lee, et al., High performance cellulose nanocomposites: comparing the reinforcing ability of bacterial cellulose and nanofibrillated cellulose, ACS Appl. Mater. Interfaces 4 (8) (2012) 4078–4086.
[32] M.N. Norizan, Development of sugar palm yarn and woven glass fibre-reinforced unsaturated polyester composites, in: Faculty of Engineering, Universiti Putra Malaysia (UPM), 2018, p. 150.
[33] K.K. Chawla, Composite Materials: Science and Engineering, Springer Science & Business Media, 2012.
[34] N.M. Nurazzi, et al., Thermal properties of sugar palm yarn reinforced unsaturated polyester composites as an alternative for automotive applications, in: Biocomposite and Synthetic Composites for Automotive Applications, Elsevier, 2021, pp. 19–49.
[35] J. Gustin, et al., Low velocity impact of combination Kevlar/carbon fiber sandwich composites, Compos. Struct. 69 (4) (2005) 396–406.
[36] N. Mohd Nurazzi, et al., Effect of fiber orientation and fiber loading on the mechanical and thermal properties of sugar palm yarn fiber reinforced unsaturated polyester resin composites, Polimery 65 (2020).
[37] K.T. Lau, et al., Properties of natural fibre composites for structural engineering applications, Compos. B Eng. 136 (2018) 222–233.
[38] V. Chinnasamy, et al., Characterization on thermal properties of glass fiber and kevlar fiber with modified epoxy hybrid composites, J. Mater. Res. Technol. 9 (3) (2020) 3158–3167.
[39] M. Idicula, et al., Dynamic mechanical analysis of randomly oriented intimately mixed short banana/sisal hybrid fibre reinforced polyester composites, Compos. Sci. Technol. 65 (7-8) (2005) 1077–1087.
[40] S.H. Aziz, M.P. Ansell, The effect of alkalization and fibre alignment on the mechanical and thermal properties of kenaf and hemp bast fibre composites: Part 1–polyester resin matrix, Compos. Sci. Technol. 64 (9) (2004) 1219–1230.
[41] N. Jesuarockiam, et al., Enhanced thermal and dynamic mechanical properties of synthetic/natural hybrid composites with graphene nanoplateletes, Polymers 11 (7) (2019) 1085.